Asian Journal of Pharmaceutical Sciences 17 (2022) 102–119

Available online at www.sciencedirect.com

ScienceDirect

journal homepage: www.elsevier.com/locate/AJPS

Original Research paper

Surface-engineered liposomes for dual-drug delivery targeting strategy against methicillin-resistant *Staphylococcus aureus* (MRSA)

Nur Najihah Izzati Mat Rani[a,b], *Xiang Yi Chen*[a], *Zahraa M. Al-Zubaidi*[a], *Hanisah Azhari*[a], *Tzar Mohd Nizam Khaitir*[c], *Pei Yuen Ng*[d], *Fhataheya Buang*[a,e], *Geok Chin Tan*[f], *Yin Ping Wong*[f], *Mazlina Mohd Said*[d], *Adeel Masood Butt*[g], *Azmy A. Hamid*[h], *Mohd Cairul Iqbal Mohd Amin*[a,*]

[a] *Centre for Drug Delivery Technology, Faculty of Pharmacy, Universiti Kebangsaan Malaysia, Kuala Lumpur 50300, Malaysia*
[b] *Faculty of Pharmacy and Health Sciences, University Kuala Lumpur Royal College of Medicine Perak No.3, Perak 30450, Malaysia*
[c] *Department of Medical Microbiology & Immunology, Faculty of Medicine, Universiti Kebangsaan Malaysia, Kuala Lumpur 56000, Malaysia*
[d] *Drug and Herbal Research Center, Faculty of Pharmacy, Universiti Kebangsaan Malaysia, Kuala Lumpur 50300, Malaysia*
[e] *Reading School of Pharmacy, University of Reading, Reading RG66AD, United Kingdom*
[f] *Department of Pathology, Faculty of Medicine, Universiti Kebangsaan Malaysia, Kuala Lumpur 56000, Malaysia*
[g] *Institute of Pharmaceutical Sciences, University of Veterinary and Animal Sciences, Lahore 54000, Pakistan*
[h] *XORIX Sdn Bhd, Dungun Terengganu 23000, Malaysia*

ARTICLE INFO

Article history:
Received 28 August 2021
Revised 26 October 2021
Accepted 26 November 2021
Available online 24 December 2021

Keywords:
Erythrocyte
Dual drug delivery
Liposome
Methicillin-resistant staphylococcus aureus
Vancomycin
Daptomycin

ABSTRACT

This study focused on the encapsulation of vancomycin (VAN) into liposomes coated with a red blood cell membrane with a targeting ligand, daptomycin–polyethylene glycol–1,2-distearoyl-sn-glycero-3-phosphoethanolamine, formed by conjugation of DAPT and N-hydroxysuccinimidyl-polyethylene glycol-1,2-distearoyl-sn-glycero-3-phosphoethanolamine. This formulation is capable of providing controlled and targeted drug delivery to the bacterial cytoplasm. We performed MALDI-TOF, NMR and FTIR analyses to confirm the conjugation of the targeting ligand via the formation of amide bonds. Approximately 45% of VAN could be loaded into the aqueous cores, whereas 90% DAPT was detected using UV–vis spectrophotometry. In comparison to free drugs, the formulations controlled the release of drugs for > 72 h. Additionally, as demonstrated using CLSM and flow cytometry, the resulting formulation was capable of evading detection by macrophage cells. In comparison to free drugs, red blood cell membrane–DAPT–VAN liposomes, DAPT liposomes, and VAN liposomes reduced the MIC and significantly increased bacterial permeability, resulting in > 80% bacterial death within 4 h. Cytotoxicity tests were performed *in vitro* and *in vivo* on mammalian cells, in addition to hemolytic activity tests in human erythrocytes, wherein drugs loaded into the liposomes and RBCDVL exhibited low toxicity. Thus, the findings of this study provide insight about a dual antibiotic targeting strategy that utilizes liposomes and red blood cell membranes to deliver targeted drugs against MRSA.

* Corresponding author.
E-mail address: mciamin@ukm.edu.my (M.C.I.M. Amin).
Peer review under responsibility of Shenyang Pharmaceutical University.

https://doi.org/10.1016/j.ajps.2021.11.004

1. Introduction

Nanotechnology has been used in various fields over the last decade, including cosmetics, food technology, and pharmaceuticals [1,2]. The imminent threat of widespread methicillin-resistant *Staphylococcus aureus* (MRSA), or in the worst-case scenario, vancomycin-resistant *S. aureus* (VRSA), has compelled pharmaceutical scientists to design and develop a long-term, cutting-edge drug delivery technology to halt the spread of antibiotic resistance. Skin and soft tissue infections account for most MRSA infections, and in some cases, bacteria can enter the circulation directly through a break in the skin or another infection site, causing bacteremia and right-sided endocarditis. A ground-breaking antibiotic drug delivery platform is in high demand for combating antibiotic resistance. Nanocarriers (NCs) such as organic/metal nanoparticles have been developed for encapsulation of biologically active drugs against MRSA [3]. Existing artificial NCs in clinical use are often recognized as foreign objects, eventually initiating immune responses, owing to their non-self-properties [4]. Hydrophilic polymers, such as polyethylene glycol, have been widely used to improve biological retention; however, their efficacy may reduce when used frequently [5,6]. Moreover, unfavorable immunological reactions to PEGylated-based formulations might be dangerous, as they could lead to the initiation of anti-PEG IgG and IgM hypersensitivity reactions [7,8], which may cause severe allergic symptoms, and in rare cases, fatal anaphylaxis [9]. For exerting the maximum therapeutic effect against MRSA, NCs such as liposomes are designed to directly target the bacteria and subsequently hinder immune system recognition for a timed release of their cargoes [10–13]. Surface modifications using various functional components and immune antagonists have enabled immune response regulation, ensuring effective treatment.

Daptomycin (DAPT) is well-known for its potent bactericidal activity against Gram-positive pathogens that are notoriously difficult to treat. It has a 13-member amino acid cyclic lipopeptide with a decanoyl side chain. The antibacterial effect of DAPT is achieved by preventing the synthesis of lipoteichoic acid (LTA), which acts as a membrane receptor or DAPT-binding molecule [14,15]. LTA works as both a regulator of muramidase and an adhesion amphiphile [16], and upon attaching to the bacterial cell wall, DAPT causes the cell membrane to be perturbed and depolarized. One hypothesis proposes that DAPT binding affects membrane fluidity, leading to the dissociation of cell wall biosynthesis enzymes such as glycosyltransferase, MurG and acyl-ACP:phosphate transacylase, PlsX [17]. According to the recent study, calcium-bound DAPT, phosphatidylglycerol (PG) and other undecaprenyl-coupled cell envelope precursors form tripartite complexes, which then incorporate lipid II. This complex is thought to prevent cell division, disrupt cell wall synthesis machinery, and finally cause membrane bilayer lysis at the septum, resulting in cell death [17,18]. Another notable hypothesis is based on early discoveries that DAPT caused potassium ion leakage and membrane potential loss in treated bacterial cells, in a calcium-dependent manner [19]. Acetyl-L-alanine and peptidoglycan are two other direct inhibitors of the cell wall/membrane; however, there are no detailed studies examining their mechanisms of action, with respect to the targeting of LTA synthesis.

MRSA in the bloodstream can secrete gamma-hemolysin, a leukotoxin with strong hemolytic activity against erythrocytes [20–22]. In the current study, the preparation of the formulation involved coating the liposomes with red blood cell (RBC) membranes to impart biomimetic effects and improve their immune-evading capability. Contact with the toxin released by MRSA would lead to the surface engineered liposomes being exposed to the targeting ligand, consisting of DAPT attached to polyethylene glycol–1,2-distearoyl-sn-glycero-3-phosphoethanolamine (DAPT-PEG-DSPE), which is capable of binding to the cell wall of *S. aureus* via its hydrophobic tail for site-specific delivery against MRSA. In the current study, we developed biological interfaces by combining liposomes and RBC membranes; the model drug vancomycin (VAN) was loaded in the inner core of liposomes and drug effect was further enhanced by loading DAPT, for achieving a dual drug delivery targeting strategy against MRSA. The surface of the developed "stealth liposome" was modified to prevent opsonization, improve systemic circulatory time, and enhance the half-life of the drugs. While treating potentially multidrug-resistant microbes, it is critical to reduce the antibiotic dosages while maintaining antibacterial activity. Thus, the dual drug delivery targeting strategy developed in this study has the potential to assist in overcoming MRSA infections and prolonging antibiotic lifespan.

2. Materials and methods

2.1. Materials

All the reagents and formulations used in the experiment were prepared with ultrapure water from a Milli-Q Plus apparatus (Millipore, Billerica, USA). The antibiotics DAPT and VAN were obtained from Cayman Chemical (Michigan,USA). We purchased NHS–PEG_{3400}–DSPE, m-polyethylene glycol2000 (mPEG2000)-DSPE, Triton X-100, dimethyl fumarate (DMF), fluorescein amine isomer II (FAM), 1,1′-dioctadecyl-3,3,3′,3′-tetramethylindocarbocyanine perchlorate (DIL), phosphate-buffered saline (PBS) tablet, and 3-[4,5-*dimethylthiazol*-2-*yl*]−2,5-diphenyltetrazolium bromide (MTT) from Sigma–Aldrich Chemie GmbH (Taufkirchen, Germany). SnakeSkin™ Dialysis Tubing [molecular weight (MW) cut off = 3500 Da] and Invitrogen™ egg yolk phosphatidylcholine (EPC) were obtained from Lipoid GmbH (Ludwigshafen, Germany); Mueller-Hinton broth (MHB) and MH were obtained from Oxoid (Hampshire, United Kingdom); Eagle's minimum essential medium (EMEM), Addexbio (San Diego, USA); SimplyBlue™ SafeStain, penicillin/streptomycin, fetal bovine serum (FBS) and trypsin-EDTA were obtained from Thermo Fisher (Gaithersburg, USA); Annexin V-APC Reagent and Annexin V Binding Buffer (10 ×) was obtained from Elabscience (Texas, USA); cell viability kit was obtained from BD Biosciences (New Jersey, USA); and the human embryonic kidney cell line HEK293, RAW 264.7, and MRSA (Mu50) were obtained from American Type Culture Collection

Table 1 – Parameters Involved in Experimental design of I-optimal (combined).

Component/Factor	Name	Unit	Type	Minimum	Maximum
A	EPC	g	Mixture	0.55	0.70
B	Cholesterol	g	Mixture	0.25	0.40
C	mPEG2000-DSPE	g	Mixture	0.00	0.05
D	Ultrasonic Intensity	%	Numeric	30.00	90.00
E	Sonication Time	min	Numeric	5.00	15.00

(ATCC; Virginia, USA). Human hepatocellular carcinoma cells (HepG2) and MRSA clinical isolates were a gift from Universiti Kebangsaan Malaysia Medical Center. All other reagents were of analytical grade.

2.2. *Synthesis and characterization of targeting compound*

To produce the targeting compound DAPT–PEG–DSPE through amide reaction, DAPT was coupled with NHS–PEG_{3400}–DSPE at a molar ratio of 1.2:1, wherein distilled DMF was used as the solvent [12]. The pH was adjusted to 8.0–8.5 with an equivalent proportion of triethylamine; the solution was stirred continuously for 72 h at 25 °C before dialysis (MW cut-off = 3500 Da) against sterile water for 48 h. Lyophilization was performed to preserve the product. To verify the coupling of DAPT with NHS–PEG_{3400}–DSPE, the product was analyzed using matrix-assisted laser desorption/ionization time-of-flight mass spectrometry (MALDI-TOF-MS; Autoflex pace, Bruker, Bremen Germany), fourier-transform infrared spectroscopy (FTIR, Perkin Elmer Spectrum 100 FTIR spectrometer, USA), and nuclear magnetic resonance (NMR; AVANCE III HD 400 MHz, Bruker, USA).

2.3. *Preparation of liposomes via experimental design*

An I-optimal (combined) design from the Design Expert® software was selected to accommodate a mixture of components and numeric or categorical factors involved in the formulation process. This flexible design incorporates one mixture (three components), two numeric factors, and two responses.

Preliminary experiments and data from existing research were used to identify and estimate the ranges of the minimum and maximum limit [23–27]. The mixture components consisted of EPC (A), cholesterol (B), and mPEG2000–DSPE (C), whereas the processing factor incorporated ultrasonication intensity (D) and sonication time (E). The effects of these five parameters were evaluated on two response variables: ζ-average (R1) and polydispersity index (R2). The total number of design points according to the I-optimal (combined) was 43. The design points included three replicated points and four lack-of-fit points. The I-optimal design (combined) had more runs in the center and focused on prediction. The formulations were prepared in random order. The design points are listed in Table 1. The validation optimal condition model was proved by repeating it six times. Moreover, 95% of the two-sided prediction intervals (95% PIs) were generated from the observed data for the validity test of the proposed models. PI is a range of values that reflects a future outcome from the same population with a predetermined confidence level. Hence in this study, the optimum level of mixture components and processing factors was established to produce liposomes with desirable responses, and we estimated that only 5% of liposomal formulation will not be included in this range.

2.4. *Preparation of liposomes using the dehydration rehydration vesicles (DRV) method*

EPC was used because it is a natural source with better oxidation stability compared to other types of lipids [28]. The mixture compositions were optimized according to the generated ratios. Liposomes were prepared according to a previously established method [29]. Briefly, EPC, cholesterol, and (mPEG2000)–DSPE were mixed at different molar ratios with chloroform in a round-bottomed flask. The organic solvent was evaporated above the transition temperature at 40 °C using a rotary evaporator for 15 min until the formation of a thin film, which was dried under vacuum for 24 h to remove remaining traces of organic solvents and mixed with physiological saline (blank liposomes) or saline containing DAPT /VAN (drug: lipid = 1:10, w/w) to produce drug-loaded liposomes. The optimized drug mass ratio of DAPT:VAN was 1:1.3, selected based on the fractional inhibitory concentration (FIC) study. The liposomes formed were further subjected to sonication using a QSONICA500 Probe Sonicator (Connecticut, USA) with a maximum power output of 500 W. After each 5 min run, the ultrasonic processor was paused for 5 min. A thermometer was used to keep track of the temperature maintained at 30 °C and adjusted using an ice-water bath.

The effects of lipid, cholesterol, mPEG2000–DSPE, and fixed DAPT-PEG-DSPE were examined on ζ-average (R1) and polydispersity index value (R2) in the same optimal processing environment. The aim was the encapsulation of the drug in the final liposomes. The mean ζ-average and polydispersity index (PDI) were analyzed using a ZetaSizer NanoZS (Malvern Instruments, United Kingdom). A dilution factor of 1:100 with PBS was used before analysis [30,31].

2.5. *Preparation of ghost erythrocytes*

Ghost erythrocytes were prepared using the hypotonic hemolysis method [32]. Whole blood was obtained via the cardiac puncture of male Sprague Dawley rats, and RBCs were separated using centrifugation (400 × *g*, 10 min), followed by three washes with cold PBS (300 mOsm, pH 7.4). The isolated RBCs were suspended in 1 ml of 0.25 × PBS hypotonic

lysis buffer and stored at 4 °C (pH 7.4). Hypotonic lysis was performed for 20 min, and the RBC-derived ghost erythrocytes were centrifuged two times at 17 000 × *g* for 5 min each time before washing with ice-cold PBS for extraction and eradication of excess hemoglobin, followed by incubation with an antibiotic-containing solvent for 2 h. Unencapsulated drugs were removed via centrifugation at 17 000 × *g* for 5 min. The ghost erythrocytes were viewed under a Nikon TS100 inverted phase-contrast microscope (Nikon Instruments, Tokyo, Japan) at 40 × magnification.

2.6. Transmission electron microscopy (TEM)

PBS was used to prepare 100-fold diluted solutions of ghost erythrocytes, VAN-L, and RBCDVL. For 90 s, the diluted samples were dropped onto a formvar carbon film-coated 300 mesh copper grids (FCF 300-Cu). Next, for another 90 s, the copper grids were immersed in a few drops of uranyl acetate (2%) solution. The grids were analyzed at 120 kV using a Tecnai G2 Spirit BioTWIN electron microscope (FEI Co., Oregon, USA).

2.7. Determination of minimum inhibitory concentration (MIC), minimum bactericidal concentration (MBC), and FIC

The broth microdilution method was used to assess the MIC of free drugs and liposomal formulations according to the Clinical and Laboratory Standards Institute (CLSI, 2009) [33]. Each formulation was applied to 96-well plates at two-fold dilutions, yielding concentrations ranging from 0.0625 to 4 μg/ml. Subsequently, 100 μl MRSA strain in MHB was applied to each well, resulting in a final inoculum of 1×10^6 colony-forming units (CFU)/ml. Ca^{2+}-supplemented Mueller-Hinton broth (50 mg/ml) was used to evaluate the MIC of DAPT [34,35]. The 96-well plates were cultured at 37 °C for 24 h. The MIC was defined as the minimum concentration of antibiotic that caused no MRSA growth after 24 h. The experiment was repeated three times.

After the MIC values were identified, a total of 10 μl from each well that showed no bacterial growth after the incubation process was spread on top of the agar plate and incubated at 37 °C for 24 h. MBC is determined when bacteria cannot grow after incubation with the test compound and cannot be rescued when plating in compound-free agar. Hence, concentrations that killed >99.9% of the bacterial population and indicated no bacterial colonies above agar after 24 h of the incubation period were recorded as MBC values. Each experiment was repeated three times.

The enhanced antibacterial effect was further assessed using BD FACSCanto flow cytometry machine (BD Biosciences, USA) [36]. At 35 °C, liposomes were combined with a bacterial suspension (1×10^6 CFU/ml) with agitation according to the MIC dose. As a control, a solvent was used to dilute the formulations. At predetermined time intervals (0, 2 and 4 h), aliquots were washed with 1 ml of PBS and centrifuged at 2000 × *g* for 5 min to remove free liposomes. Bacteria and liposomes attached to the bacteria were included in the pellet, while the remaining supernatant contained free liposomes. For the flow cytometry study, the bacterial pellet was diluted in 200 μl PBS. Labeling using an equal amount (5 μl) of propidium iodide (PI) and thiazole orange (TO) was used to monitor bacterial viability.

The dynamic checkerboard procedure was used in 96-well plates, with two-fold dilutions of DAPT-L and VAN-L dispensed in a checkerboard pattern [37]. For each liposome, the serial concentrations of DAPT-L and VAN-L ranged from 1/64 to 1 × MIC. Bacterial inoculum was added (1×10^6 CFU/ml). The FIC index was determined after 24 h incubation at 37 °C [38].

2.8. Determination of encapsulation efficiency (EE)

EE was calculated using the percentage difference between the total antibiotic (encapsulated and nonencapsulated) and the free antibiotic. The lyophilized liposome powder was used to efficiently encapsulate the VAN into liposomes to generate liposomal VAN. Then, with a weight ratio of VAN to liposomes of 1:10, VAN was added to the lyophilized powder of liposomes. The following formulas were used to calculate the EE and drug loading capacity (DLC):

$$EE\ (\%) = \left(\frac{Wt}{Wi}\right) \times\ 100\%$$

$$DLC\ (\%) = \left(\frac{Wt}{Wo}\right) \times\ 100\%$$

where *Wt* is the total mass of the drug loaded in liposomes, *Wi* is the total mass of the drug (VAN or DAPT) initially added during preparation, and *Wo* is the total mass of the purified liposomes containing the drug (VAN or DAPT).

Liposomal formulations and the RBC-coated liposomes were ruptured by the membrane-disruption method using 2% Triton X-100 [39]. The amount of drug released was determined using the GENESYS™ 180 UV-Visible Spectrophotometer (Thermo Scientific™, USA). Absorption was measured at 280 nm for VAN and 221 nm for DAPT. Increased antibiotic concentrations indicated further disruption, while lower antibiotic concentrations suggested that certain liposomes did not completely release their contents. The absorbance readings were converted to concentration values using a calibration curve created specifically for each antibiotic to determine concentration based on absorbance.

2.9. Encapsulation confirmation via flow cytometry

Flow cytometry was used to validate the successful encapsulation of RBCDVL and VAN-L [32]. RBCs were washed twice with ice-cold PBS. The percentage of the volume of RBC membrane accessible by liposomes in preparation before incubation was determined by mixing the same volume of RBC membrane preparation and liposome preparation. Liposomes loaded with fluorescent probes were prepared using a procedure similar to that used to produce liposomes containing VAN and DAPT, with VAN replaced by FAM (Ex/Em, 493/517 nm) and DAPT by DIL (Ex/Em, 549/565 nm). To determine the EE, 5 μl FAM/DIL was dissolved in chloroform with a mixture of EPC, cholesterol, mPEG2000-DSPE, and DAPT-PEG-DSPE before being subjected to evaporation and drying under vacuum. Rehydration was subsequently

performed with the FAM solution before incubation with the RBC membrane to allow the transition of liposomes loaded with VAN into the RBC membrane's pores across the concentration gradient. The RBC membrane was suspended in 1 × PBS to close the pores and then centrifuged at 400 × *g*. The RBC membrane was washed three times with cold PBS and centrifuged at 400 × *g* for removing unloaded drug molecules. The supernatant was removed, and the pellets were collected and diluted with 200 µl of isotonic solution. The final formulation results were validated using the BD FACSCanto flow cytometry machine and TEM imaging.

2.10. Cumulative drug release of VAN and DAPT

We used the dialysis method to investigate the kinetics of *in vitro* drug release [38]. DAPT-L/VAN-L, RBCDVL (2 ml, donor solution) was placed into a dialysis tube (MW = 3500 Da) and immersed in 30 ml PBS solution at pH 7.4. For DAPT-based formulations, 50 mg/ml Ca^{2+} was added as the release medium. The medium was stored at 37 °C under continuous magnetic stirring at 100 rpm. At predetermined time intervals (0, 2, 4, 6, 8, 12, 24, 48, 96, 120 and 144 h), 200 µl the receiver solution was collected, and the same amount of new medium was replaced. The percentage of drugs obtained was analyzed using a UV spectrophotometer, and these tests were performed in triplicate. The calculated average values were used to express the results as the mean ± standard deviation (SD).

2.11. Stability study of liposomes after reconstitution

The effect of temperature on the stability of the optimized liposomal formulation was studied by storing the formulations after reconstitution at 4 ± 2 °C for 21 d [40]. All formulations were sterilized with a 0.22 µm nylon syringe filter (Merck & Co., New Jersey, USA) and filled in an autoclaved glass sample bottle before storage. Morphological changes of the formulations were observed at several time points (0, 14 and 21 d) by TEM imaging, as described in Section 2.6.

Another method for evaluation of stability involved determining the presence of proteins in the RBCDVL via sodium dodecyl sulfate–polyacrylamide gel electrophoresis (SDS-PAGE) with Coomassie Brilliant Blue staining on Days 0, 14 and 21. RBCDVL was prepared as per the procedure described previously and placed in an Eppendorf tube before centrifugation at 13 000 × *g* for 5 min. The supernatant was removed, and the pellets were washed with cold PBS containing 2 mM EDTA and left for 60 s before being subjected to a re-centrifugation process. Cell pellets were re-suspended in 50 µl radio immune precipitation assay buffer (RIPA, Merck & Co., New Jersey, USA) containing protease and phosphatase inhibitor (Pierce) for 30 min on ice. The mixture was re-centrifuged at 13 000 × *g* for 15 min at 4 °C. Cell supernatants were collected and evaluated using the Bradford assay to determine protein concentration in the cell lysate: protein standard curves were constructed using bovine serum albumin (BSA) (Bio-Rad, USA) diluted in distilled water at different concentrations (15.6, 31.25, 62.5, 125, 250, 500 and 1000 µg/ml). Cocktails (100 µl) containing phosphatase inhibitors (PIC) and RIPA (1:99; v/v) were inserted into cell pellets and pellet dissolution was performed repeatedly with the tip of a pipette on ice before incubation for 10 min. SeeBlue Plus2 Pre-staining (Thermo Fisher, USA), served as a molecular ladder. Electrophoresis was performed at 100 V for 1.5 h in a TBST running buffer (Bio-Rad, USA).

The gel was rinsed with 100 ml of ultrapure water three times for 5 min. Water was removed from each rinse, and the gel was stained with SimplyBlueTM solution (approximately 20 ml) until the gel was covered for 1 h at room temperature with moderate shaking (YR407 / YR406 Orbital Shaker, Kalstein, France). We rinsed the gel two times with 100 ml of water for 1 h to increase the intensity of the band and reduce the background.

2.12. Macrophage uptake

Flow cytometry and fluorescence microscopy were used to assess the macrophage uptake [41]. RAW264.7 Cells (ATCC TIB-71) were cultured in a complete growth medium (DMEM). The cells were split at 80% confluency, and after separation, the cells were seeded into 6-well plates (10^5 cells/well) in a cell culture medium. After 24 h, the medium was replaced with a serum-free medium. VAN-L, DAPT-L and RBCDVL were added to the cell culture medium, and the mixture was incubated for 2 h at 37 °C. The cells were then detached using 2.5% trypsin for flow cytometric analysis.

For experiments using confocal laser scanning microscopy (CLSM), RAW264.7 cells (10^5 cells) were seeded in ibidi Treat µ-dishes (ibidi GmbH, Germany) for 24 h. Next, at 50 µg/ml concentrations, formulations encapsulated with a fluorescent dye or coated with an antibody were added to be cell culture and incubated for 2 h. PBS was used to wash the cells before analysis.

2.13. Cytotoxicity

Human RBCs were used to test the hemolytic activity of liposome formulations based on a previously established protocol [42]. Fresh blood samples were inserted into tubes containing EDTA to prevent coagulation. The sample was then flushed at a speed of 750 × *g* for 15 min and washed with sterile PBS three times for serum separation. The serum was replaced with the same quantity of sterile PBS for preparation of 1% RBC suspension. Each formulation (100 µl; final concentrations = 1 mg/ml, 0.5 mg/ml, 0.125 mg/ml) was combined with 100 µl RBC into a microcentrifuge tube and incubated using an incubation shaker at 37 °C for 2 h. Triton X-100 (0.5%, v/v) was selected as the positive control, while sterile PBS was used as a negative control. After incubation, all samples were dispersed at 750 × *g* for 15 min. Then, 50 µl supernatant was collected and placed on a 96-well plate. Absorbance was read at 540 nm using a microplate spectrophotometer (NanoQuant Infinite M200 PRO, Tecan, Switzerland); the measurement was repeated three times.

MTT-based toxicity studies were conducted on two cells, HEK293 and HepG2, according to a previously reported method [43]. HEK293 and HepG2 cells were cultured in a complete growth medium (EMEM) at 37 °C with 5% CO_2. The cells (200 µl per well; concentration adjusted to 1.0×10^4 cells/well) were incubated in a 96-well plate for 24 h with 5% CO_2 at

37 °C to promote cell adhesion. Each formulation produced was diluted in series at concentrations in the range 0.00469–0.6 mg/ml using EMEM. After 24 h, the old media in each cell well was replaced with 200 µl media containing the formulation. The experiment was conducted at intervals of 24, 48 and 72 h. After the incubation period at each specific time, the old media was removed and replaced with 20 µl 5 mg/ml MTT and re-incubated for 4 h. Then, MTT was replaced with 100 µl DMSO to dissolve the resulting formazan crystals. Untreated cells were used as the negative control, while the free antibiotics DAPT and VAN were used as positive controls. Empty liposomes and RBC membranes were used as normal controls. Absorbance was measured at 570 nm using a microplate spectrophotometer.

2.14. *Biodistribution study*

All animal experiments were conducted in compliance with the guidelines for the care and use of laboratory animals published by the National Institutes of Health. Biodistribution studies were performed as outlined by Hu et al. [44], with slight modifications [12,45]. Twenty-eight male Sprague Dawley rats (6–8 weeks old) from the Laboratory Animal Resource Unit, Faculty of Medicine University Kebangsaan Malaysia (UKM) were randomly assigned to two groups: those treated with FAM-loaded liposomes alone and those administered liposomes with RBC membrane coating intravenously. In each group, the dosage was equivalent to approximately 92.5 mg/kg VAN. Rats were sacrificed by cardiac puncture, and the spleen, liver, kidney, brain, heart, and lungs were harvested at predetermined intervals (24, 48 and 72 h). The organs were weighed carefully and homogenized in 1 ml PBS. The overall blood weight of the rats was 6% of their body weights. A Synergy™ HTX Multi-Mode Microplate Reader (BioTek Instruments, USA) was used to calculate the fluorescence intensity of each sample.

2.15. *In vivo safety evaluation*

We used a completely automated biochemical analyzer to perform a preliminary safety evaluation of the formulations by examining the biochemical parameters related to alanine aminotransferase, creatinine, aspartate aminotransferase, uric acid, and blood urea nitrogen (TMS-1024i, BOEKI, Japan).

Two groups were used in the *in vivo* cytotoxicity study, wherein six treatment groups of 72 Sprague Dawley rats ($n = 6$) were administered a single-dose treatment via tail vein with one of the following preparations: DAPT-L, VAN-L, RBCDVL, or saline. The dose of DAPT-L or RBCDVL was approximately 25 mg/kg DAPT, which is less than half of the previous dose [46]. Normal rats were administered saline injections into the tail vein. Kidney and liver samples were obtained on the third day post-injection from the rats receiving VAN, DAPT, VAN-L, DAPT-L, RBCDVL, and saline. Histological analysis was performed by two independent pathologists using a Nikon Eclipse Ci microscope (Nikon Instruments, Japan).

2.16. *Ethical declaration*

The experiments involving animals, including the method of withdrawing blood and preparation of ghost erythrocytes, was approved by the animal ethics committee of Universiti Kebangsaan Malaysia (FF/2019/CAIRUL IQBAL/24-JULY/1023-AUG. 2019-AUG.–2020).

3. Results and discussion

3.1. *Synthesis and characterization of targeting compound*

DAPT contains an active amino group that may interact with succinimide to produce the target compound DAPT-PEG-DSPE. The process of synthesis involves conjugating DAPT (MW = 1620.68 Da) with NHS-PEG_{3400}-DSPE in DMF through an amide bond formed by a nucleophilic substitution reaction [12]. The experimental MWs determined by MALDI-TOF-MS for NHS-PEG_{3400}-DSPE and DAPT-PEG-DSPE were approximately 3700 and 5300 Da, respectively (Fig. 1). These observed values were in line with the theoretical MW, confirming the identity of the synthesized product.

From the FTIR spectra (Fig. S1), it was inferred that the incorporation of DAPT with NHS-PEG-DSPE was successfully conjugated via covalent bonding because all the relevant peaks of DAPT and NHS-PEG-DSPE were present in DAPT-PEG-DSPE. For DAPT, the peaks at 3311.6, 2346.6, 1651.30, and 1531.63 cm^{-1} correspond to –NH str., >C=NH+ str., >C=O str. of $-CONH_2$ and amide II of the primary amide linkages, respectively. The >C=NH+ linkage arising from the resonance contribution of the amide group appeared in the DAPT-PEG-DSPE spectrum because DAPT and PEG-DSPE formed an amide linkage.

The conjugation was further confirmed by NMR for molecular recognition (Fig. S2-S4). From the NMR spectrum, the presence of DAPT in the conjugated moiety, DAPT-PEG-DSPE, can be confirmed from the specific peaks of DAPT. In DAPT, the aromatic rings, benzene, and indole rings present values in the region 6.80–7.34 ppm, which are also present in DAPT-PEG-DSPE, in addition to PEG-DSPE-specific peaks. The conjugation of DAPT with NHS-PEG_{3400}-DSPE, generating an $NH–CH_2$ linkage [47], can also be confirmed based on the peaks in the region 3.46–3.67 ppm, which were absent in peaks for PEG-DSPE [48] and present in those for the conjugated moiety, while the $NH–CH_2$ peak, which was inherent for DAPT, was present at 3.76 ppm. Hence, from both NMR and IR, the conjugation of DAPT with NHS-PEG_{3400}-DSPE was verified. The degree of substitution (DS) of DAPT in the DAPT-PEG-DSPE targeting ligand was reported to be 28%.

3.2. *Preparation of liposomes via experimental design*

Response surface methodology (RSM) is a set of statistical and mathematical techniques for establishing, enhancing,

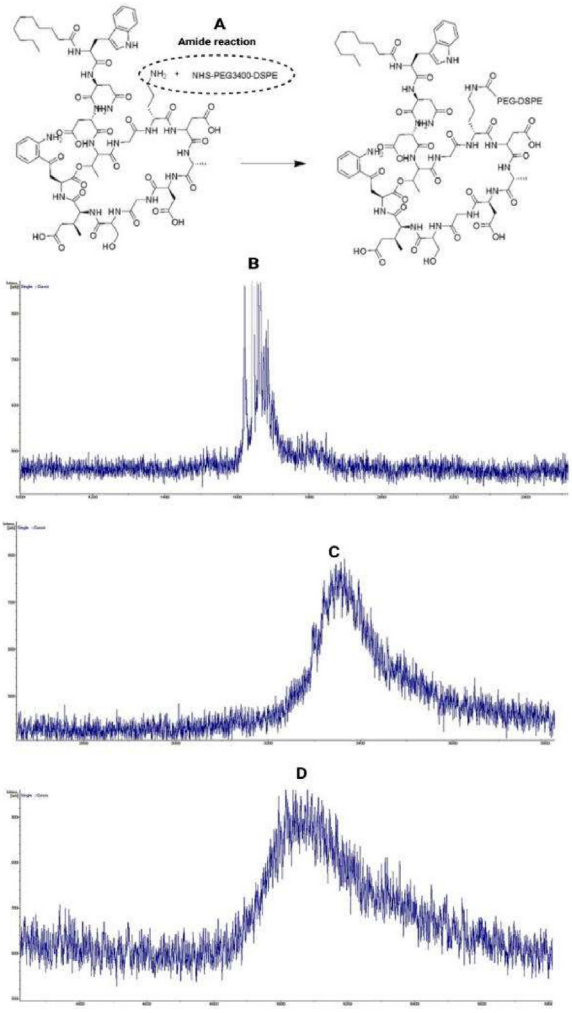

Fig. 1 – (A) Synthesis of targeting components DAPT-PEG-DSPE by amide reaction. The molecular weight of each component and the final conjugation were determined by MALDI-TOF mass spectrometry analysis. (B) DAPT was confirmed at MW 1620.68 Da. (C) NHS–PEG3400–DSPE at MW 3400 Da. (D) Formation of DAPT–PEG–DSPE with an approximate molecular weight of 5300 Da, similar to the sum molecular weights of the two components.

and optimizing processes. Processes involved in multistep pharmaceutical products greatly benefit from RSM, as they reduce the cost and time from the limitation of one factor at time approach during optimization. In this experiment, the I-optimal (combined) design was used to minimize the prediction variance over the experimental conditions while maintaining efficient runs [49].

Liposomes can be designed for the treatment of bacterial infections and delivery of biologically active components into bacteria by fusion with bacterial membranes, thus enhancing the bactericidal activity of entrapped antibiotics. The driving factor in liposome–bacteria fusion is the existence of the bacterial membrane; divalent cations, pH, liposome fluidity, and temperature affect the rate and degree of fusion. Nevertheless, liposome size is an equally crucial aspect in determining the clinical success of the formulation. Considering that the size of *S. aureus* cells (< 1.6 μm) is notably smaller than that of eukaryotic cells [50], it may be essential to regulate the size of liposomal particles for improving liposome fusion. Previous studies indicated that liposomes with particle size < 100 nm interact less with plasma proteins, thus avoiding uptake by the reticuloendothelial system (RES) and increasing its shelf life in the blood, while larger liposomes are eliminated faster from the circulatory system [51]. However, the drawback of the small size of liposomes is their limited drug storage capacity.

As high VAN concentrations should be used to achieve therapeutic effects in the MRSA infection area, the liposome size selected is generally approximately 100–200 nm. According to the average reaction result from 43 trials for particle size, ζ-average was 100–674.86 nm and the polydispersity index value was 0.0396–0.794. The DOE program proposes a model based on the selection of the highest polynomial, and the quadratic × quadratic model was selected because it corresponded to the ζ-average and value of the polydispersity index. The forecast R-squared (R^2) statistics show the amount of variability in the new data, which can be explained by the model. The final model used for the two reactions is presented in Table S1. When several reactions are considered simultaneously, the response variables must not be analyzed individually to avoid a possible correlation of reactions [52].

The first step involved in model selection and fitting is performing an ANOVA and selecting the appropriate model type. R^2 was used as a measure of fit of the model (Table S1). Based on the fit statistic summary, the final reduced quadratic × quadratic model was determined to be appropriate for navigating the design space. The adjusted and predicted R^2 values were in reasonable agreement, wherein the difference between both was less than 0.2. The non-significant lack-of-fit (LOF) test is suitable, as it compares the deviation of actual points from the fitted model.

Among sonication, extrusion, and high-pressure homogenization [26], ultrasound produced via an ultrasonic end processor is used to reduce the liposome size because it is more convenient than other methods. Exposure to ultrasound or sonication is widely used to produce liposomes; however, little is known regarding the mechanism of liposomal formation related to ultrasound. The oscillation or cavitation of small gas bubbles in various fields of pressure is responsible for most of the biophysical impact of ultrasound on cells [53]; hence, the greater the volume of streaming from the ultrasound source, the better the mixing, and consequently, homogeneity of the solution. The results of the investigation on the parameters used for sample preparation, the total mixture components of cholesterol (B), mPEG2000-DSPE (C), and processing factor, ultrasonic intensity (D), played a significant role in obtaining the ζ-average value as desired. In contrast, for PDI, the same mixture components were significant except that the processing factor affected was the sonication time (E). As shown in Fig. 2, to obtain the average size at the optimal level of 100 nm, the sonication time range proposed by the model is 9–11 min, while the best ultrasonic intensity was in the regulation range of 70%–80%. For the polydispersity index, Fig. 3 shows that to obtain a

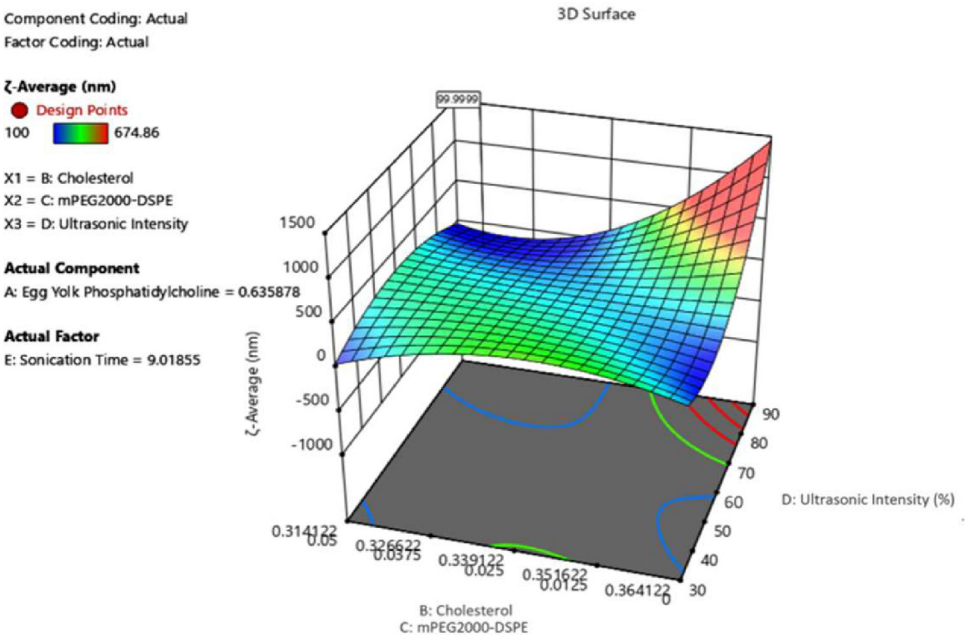

Fig. 2 – The 3D surface of mixed components and processing factors at ζ-average.

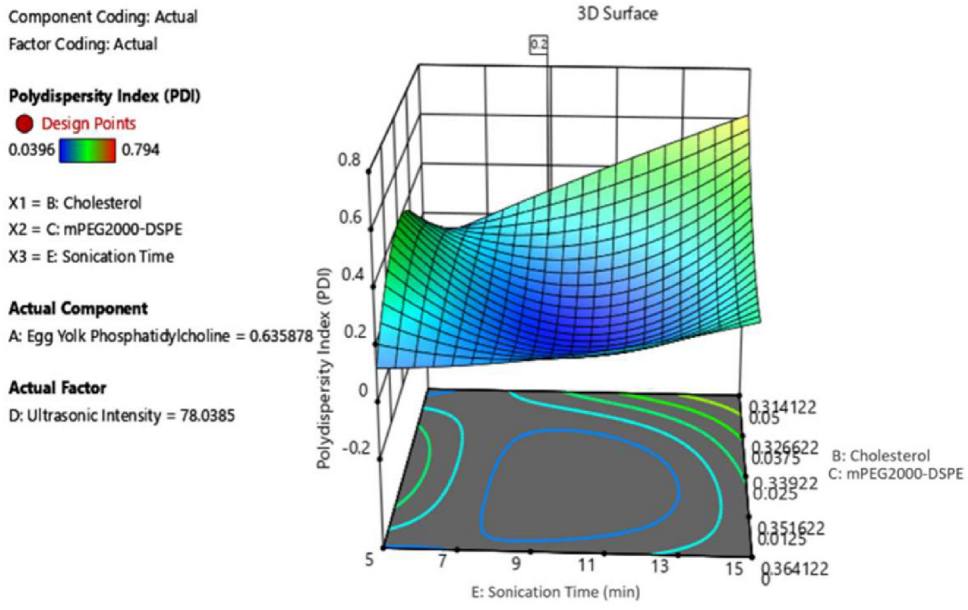

Fig. 3 – 3D surface contour plots of mixed components and processing factors at PDI.

0.2 PDI, the best ultrasonic time is 9–11 min, with 70%–80% ultrasonic intensity. During the ultrasonication process, the liposome is exposed to energy-efficient ultrasonic waves, which capable of breaking down large-sized liposomes into smaller ones. The results of this study are consistent with those of a previous study [27].

3.3. *Formulation optimization and validation test*

The desirability function in the Design Expert® software (version 12.0.) was set to be in the range for each component in the mixture, the response target of ζ-average of 100 nm with no specific PDI target. The program suggested several solutions with different combinations of mixtures and process parameters. The combinations chosen for the optimized formulation are shown in Table S2. The validity of the response surface models was confirmed, as all measured values of the three responses were within their 95% PIs.

The production of liposomal formulations using RBC membrane coatings as camouflage requires a lack of physical and chemical interactions with cell membranes to prevent load leakages that lead to toxicological problems. Therefore, liposomes must be created at the nanoscale and have high stability, and membranes must be used as a biomimicking-

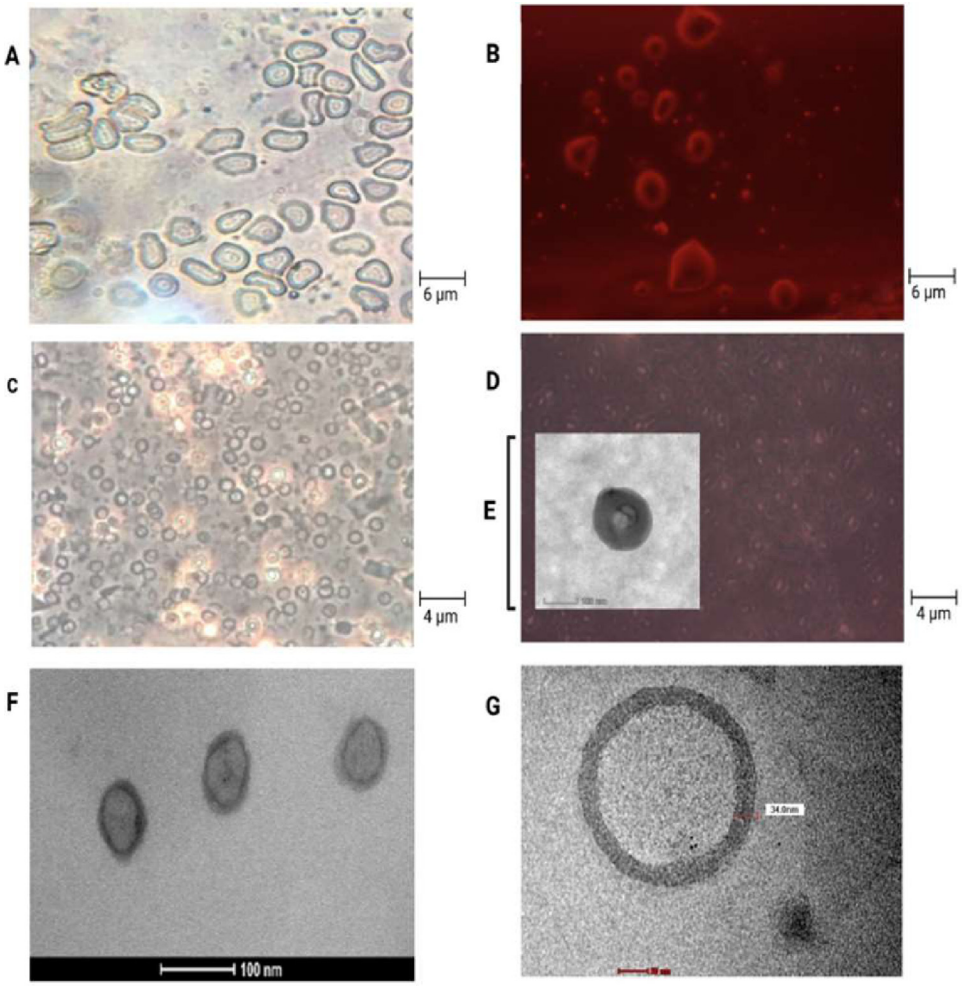

Fig. 4 – Images of liposome production and RBC membranes that use as a disguise concealing for the dual antibiotic delivery strategy against MRSA. (A) Image of RBC through an inverted microscope at 40 x magnification. (B) The use of colored contrast on red blood cell image. (C) Formation of ghost erythrocytes (D) The use of red contrast showed the formation of pores on the RBC. (E) Resulting pores on a scale of 100 nm via TEM imaging (F, G) Morphology and uniformity of liposome size produced by the dehydration-rehydration method.

based strategy to avoid being targeted by the immune system. The selection of an appropriate method, for preparing RBC membranes, contributes to maintaining biomarkers; thus, the process for membrane production in this study did not use chemicals aggressively. Liposomes produced using EPC were selected owing to their natural source. The use of TEM, in addition to dynamic light scattering analysis, can provide an estimate for liposome measurements. All liposome morphologies obtained via TEM negative staining imaging were spherical. The liposomes showed an absence of aggregation, uniform size, and narrow distribution (< 200 nm) with an EE of 39.76% ± 6.17% (VAN) and 86.65% ± 6.13% (DAPT) in RBCDVL. In addition, RBC membranes were identified via TEM and observation under an inverted microscope because of their biconcave shape and the existence of pores formed due to immersion in a hypotonic solution (Fig. 4). The optimized liposomes were then used as NCs for encapsulating dual drugs and coated with the RBC membrane (Fig. 5), owing to which triple layers were observable; the layers were denoted as follows: RBC membrane (outer layer), liposomes (second layer), and the loaded drugs existing in the core. The characterization of all formulations is reported in Table 2.

The low EE of VAN could be explained by the fact that VAN is a very hydrophilic antibiotic [54,55]. Despite employing various strategies [56], prior studies have managed to yield an EE of 9% for conventional liposomes and 13% for PEGylated liposomes. An identical EE result of 9% was also noted by Pumerantz et al. [54]. The EE achieved for VAN in the current study liposomes is similar to that established by Liu et al. (40.78% ± 2.56%) [57]; however, the EE achieved in the current study is slightly higher (45.36%±4.17%).

Another method to improve stability is the modified reverse-phase evaporation (MRPE) method to generate liposomes, which provides a wide internal aqueous area that is appropriate for encapsulating hydrophilic medicines [58]. To improve the EE, the hydration period in the MRPE method was decreased, and a microinjector was used to increase liposomal dispersion. The impact of each component, such

Table 2 – Characterization and encapsulation efficiency of all formulations produced by using DRV method. Data were expressed as mean ± SD, $n = 3$.

	ζ-average (nm)	PDI	ζ-potential (mV)	EE (%)	DL (%)
Blank Liposome	108.13±1.16	0.21±0.10	−5.42±0.96	–	–
VAN-L	128.00±0.77	0.12±0.02	−7.46±0.85	45.36±4.17	5.99±0.44
DAPT-L	124.53±0.99	0.15±0.01	−5.00±0.91	90.53±3.90	12.00±0.61
RBCDVL	176.80±3.47	0.32±0.01	−7.69±0.21	39.76±6.17(VAN) 86.65±6.13(DAPT)	5.04±0.89 (VAN) 11.04±0.99(DAPT)

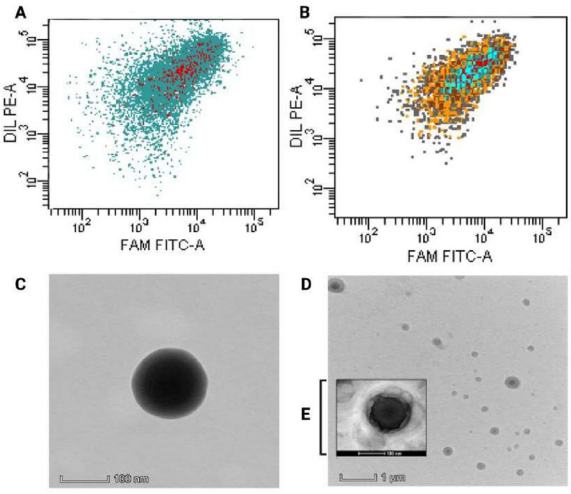

Fig. 5 – Characterization and validation of the efficiency of drug encapsulation into the resulting formulation. Flow cytometer data showed (A) VAN-L and (B) RBCDVL. TEM imaging of (C) VAN-L and (D, E) RBCVL formulations, in which red blood cell membranes appear to coat the produced liposomes and are around 20–40 nm in size.

as the cholesterol-to-lipid or drug-to-lipid ratio, on the EE of the medication encapsulated in liposomes can be assessed using RSM or an artificial neural network (ANN) [59,60].

3.4. *Cumulative drug release and stability assessment*

The *in vitro* release profiles of the VAN solution, VAN-L, DAPT-L, and RBCDVL were investigated in PBS at 37 °C (Fig. 6). All formulations showed initial bursts; for example, VAN-L released almost 50% of its content within the first 4 h, which was consistent with the number of unencapsulated drugs. Sixteen percent of DAPT was also released from DAPT-L with an EE of 90.53% ± 3.90%. Thus, it can be concluded that the drugs released in the first 4 h were drugs that could not be loaded into the resulting formulation. This also shows that dialysis is a viable albeit time-consuming approach for cleaning formulations by filtering the content across a membrane to separate the unencapsulated drug from an encapsulated drug [39]. After the cleaning steps, all formulations released residual drugs in a steady stream before plateauing. In the subsequent time interval, 84.55% ± 0.99% and 77.27% ± 0.88% of VAN was released from VAN-L and RBCDVL, respectively, and 88.2% ± 2.57% and 84.15% ± 1.27% of DAPT was released from DAPT-L and RBCDVL, respectively. However, owing to charge deposition on the membrane [61] and the physical barrier of NCs [62], drug release does not occur entirely. The presence of VAN in the liposomal core makes it difficult for this antibiotic to cross the lipid bilayer, as opposed to the DAPT conjugated to the membrane. RBCDVL and RBCDVL displayed a reasonable time-dependent, sustained-release behavior, which was attributed to the double coating of the liposome vesicles and RBC membranes. These data suggest that coating with RBC membranes can be utilized to mimic the natural circulating RBCs, thereby avoiding recognition of the RES and improving the targeting efficiency of VAN and DAPT to the site of bacterial infection.

The physical stability of the obtained NCs was further evaluated by examining morphological changes via TEM and SDS-PAGE after reconstitution. On Day 0, the liposomal formulation was considerably more polydisperse compared to Day 14 and above, and aggregation had begun. Aggregation of liposomes, which might occur because of liposomal leakage of drugs, indicating hydrolytic lipid degradation [63], can be visualized via imaging. Ester-linked hydrocarbon chain lipids are more susceptible to acids; therefore, base hydrolysis will disrupt the membrane and render the liposome conformation, which may cause the fusion of vesicles in the solution. The presence of surface proteins in the formulations was further confirmed by SDS-PAGE, performed over 21 d The presence of protein bands was clear on Day 0 and slowly faded from Day 14 to Day 21 when compared to the RBC membrane, most likely because of the leakage of the formulation, which eventually rips off the essential protein markers on the surface of the RBC [45].

To improve the stability of the liposomes, further studies need to be performed by incorporating glycerol and using various carbohydrates such as lactose, maltose [64], sucrose, mannitol, trehalose, and mannitol as cryoprotective agents [65,66]. Saccharides can maintain the liposomal membrane integrity during liposome dehydration or rehydration, and thus, are more preferred [67]. The prevention of liposomal fusion or disintegration during freezing and rehydration processes is accomplished via the establishment of a stable glassy state and connection between the polar head groups of phospholipids and sugars [68,69]. Nevertheless, optimization of the type and concentration of lyoprotectant/cryoprotectant in the formulation is required, as a higher amount of saccharides may result in instability and may lead to further drug leakage [66].

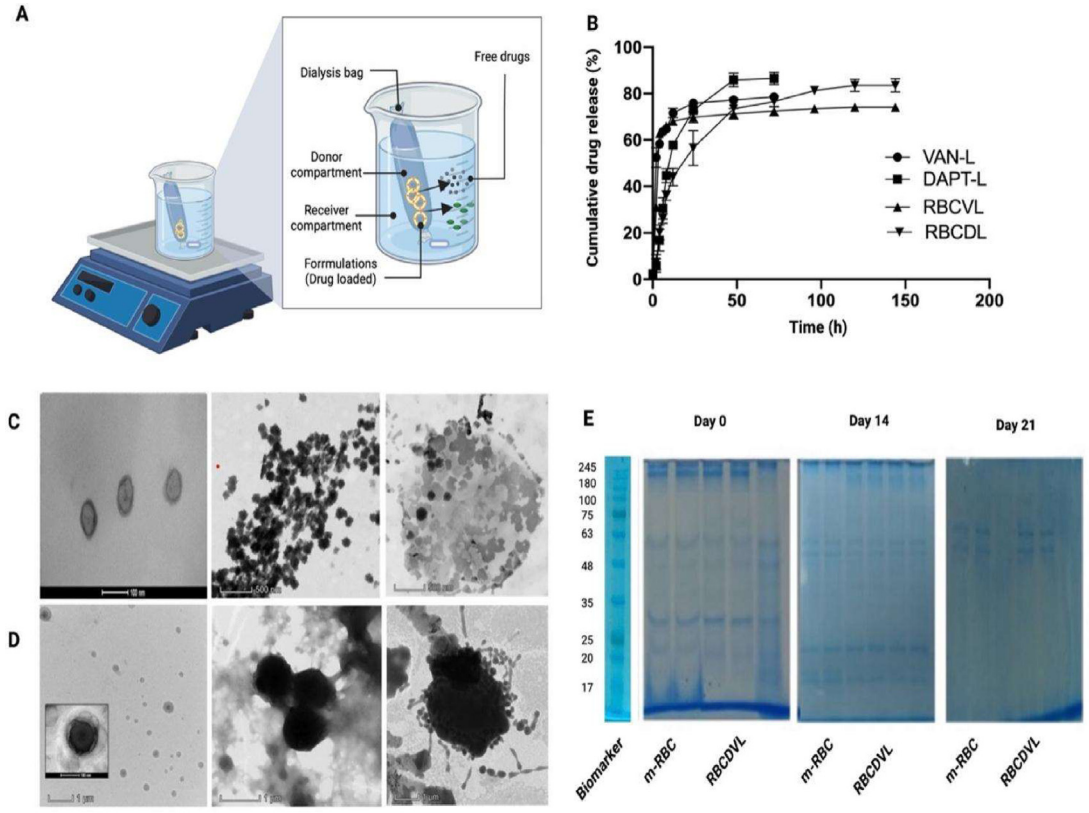

Fig. 6 – Cumulative drug release and stability assessment of formulations developed. (A) Schematic illustration of drug release. (B) The drug release profile of VAN-L, DAPT-L, RBCVL, RBCDL. *In vitro* stability was performed by TEM and SDS-PAGE on Day 0, 14, 21. (C) TEM images of liposomal preparation starting to aggregate and causing an increase in the particle size. (D) RBCDVL displayed the same character as liposomal formulation might be due to the leakage of the drug itself. (E) Relative to the fresh preparation, the surface protein band starts to fade from Day 14 onwards. Data were expressed as mean ± SD, $n = 3$.

Table 3 – MIC, MBC and FIC of free drugs and each formulation against MRSA.Data were expressed as mean ± SD, $n = 3$.

	MIC/MBC (μg/ml)					$MIC_{combined}$ (μg/ml)	Synergism Ratio	FIC** Index
	VAN	VAN-L	DAPT	DAPT-L	RBCDVL			
MRSA*(Mu50)	1.0	0.75	1.0	0.75	0.25	–	–	–
						–	–	–
MRSA*clinical isolates (blood)	1.5	1.0	1.0	0.75	0.50	0.1875 (DAPT-L)	4 (DAPT-L)	0.25
						0.25 (VAN-L)	4 (VAN-L)	0.25

* Methicillin-resistance *Staphylococcus aureus*.

** FIC = [($MIC_{combined}$ *of drug* A/MIC_{alone} *of drug* A) + ($MIC_{combined}$ *of drug* B/MIC_{alone} *of drug* B)]. FIC index of ≤0.5 indicated synergistic effects.

3.5. *MIC, MBC, FIC, and cytotoxicity*

A low-dose liposomal formulation can provide better VAN penetration into eukaryotic cells than free VAN, thereby targeting intracellular and extracellular MRSA [36]. The MIC findings in a study by Sande et al. demonstrated that liposomal VAN was twice as effective as free VAN [70]. The results obtained in the current study are concordant with those in clinical literature, wherein a low dose of VAN and daptomycin liposomes yielded an amplified antibacterial activity (lower MIC), compared to the free form (Table 3). The findings were identical for RBCDVL, which may be attributed to a dual drug targeting strategy that increases bacterial specificity. Lysis of the bacterial cell wall occurs when daptomycin binds to the bacterial surface, thus accelerating VAN release, leading to the intensified effect of VAN. Moreover, there was no bacterial recovery throughout the full incubation period in the MBC assay when disseminated on an agar plate, suggesting that the liposomal formulation exhibited antibacterial activity for a longer period than free drugs. The results of flow cytometry confirmed the liposome-bacterium interactions indicated

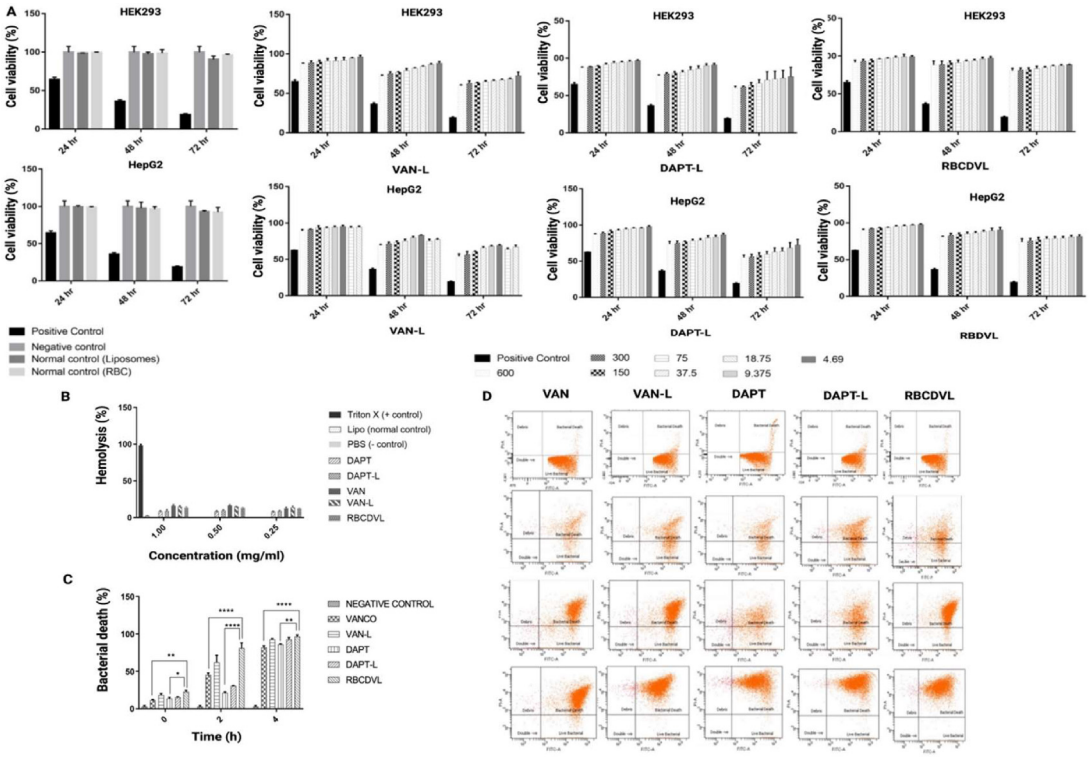

Fig. 7 – Cytotoxicity of formulations towards mammalian cells and antibacterial activity against MRSA. (A) VAN-L, DAPT-L and RBCDVL showed more than 80% cell viability than the free drugs. The drug carriers (normal control) can be considered safe with only *a* <10% reduction reported in HEK293 and HepG2 cells. Data were expressed as mean ± SEM, *n* = 3, (B) All the formulations showed low hemolysis to the human cells compared to the positive control. Data were expressed as mean ± SD, *n* = 3 (C) Enhanced antibacterial activity was observed when comparing RBCDVL to the control group, VAN and DAPT. Data were expressed as mean ± SD, *n* = 3; one-way ANOVA followed by post-hoc Dunnett or Tukey's multiple- comparison test, *P<0.05, **P<0.01, ***P<0.001 and ****P<0.0001.

by the percentage of bacterial death, which increased during the incubation period. The bactericidal effect of targeted and RBC-coated liposomes was significantly higher than that of free drugs, with VAN-L, DAPT-L, and RBCDVL killing more than 50% of bacteria in 2 h and about 80%–90% of bacteria in 4 h, whereas free DAPT and VAN killed < 50% of bacteria in 2 h (Fig. 7). Compared to free drugs, RBCDVL showed maximal membrane disruption, in addition to enhanced bacterial death, within 4 h, which might be attributable to efficient targeting and penetration of bacterial cells ($P < 0.0001$). While both forms achieved bacterial eradication within 24 h, VAN and DAPT concentrations were considerably lower in encapsulations than in the free form.

In managing MRSA, VAN is considered the mainstay treatment, despite the side effects of systemic VAN therapy. The rate of hemolysis activity was determined to evaluate the safety of the developed formulation against human RBCs. Formulations with hemolysis values <10% were considered non-hemolytic, while those with values >25% were considered at risk of hemolysis [71]. Even when tested at the highest concentrations, all formulations showed negligible hemolysis activity (less than 5%). In cytotoxicity studies, low toxicity was recorded in mammalian cells, HEK293, and HepG2 until 72 h, which is in agreement with the results of Liu et al., wherein the encapsulation of VAN inside the liposomes reduced drug-induced toxicity [57].

3.6. *Macrophage uptake*

The effect of various formulations, having FAM and DIL entrapped, on macrophage cell uptake (RAW264.7) were evaluated via flow cytometry and CLSM. Decreased macrophage uptake reduces immune system clearance, leading to a longer circulation time in the bloodstream, with a greater likelihood of the NC reaching its target location. Incubation with VAN-L, DAPT-L, and RBCDVL reduced macrophage uptake by < 10% compared to incubation with the free drugs, suggesting that inhibition of scavenger receptor-mediated uptake could lead to decreased cellular uptake, as reported previously [72]. PEG may block the scavenger pathway and reduce the cellular uptake of liposomes [29]. In addition, when compared to DAPT-L and VAN-L, RBCDVL was barely internalized by the macrophage cells, suggesting that the RBC membrane coating could successfully resist immune cell recognition (Fig. 8). Opsonins such as immunoglobulins (antibodies) and other blood proteins (*e.g.*, laminin and fibronectin), as well as complement proteins, are adsorbed onto the surface to initiate phagocytosis [73]. Related ligand-receptor

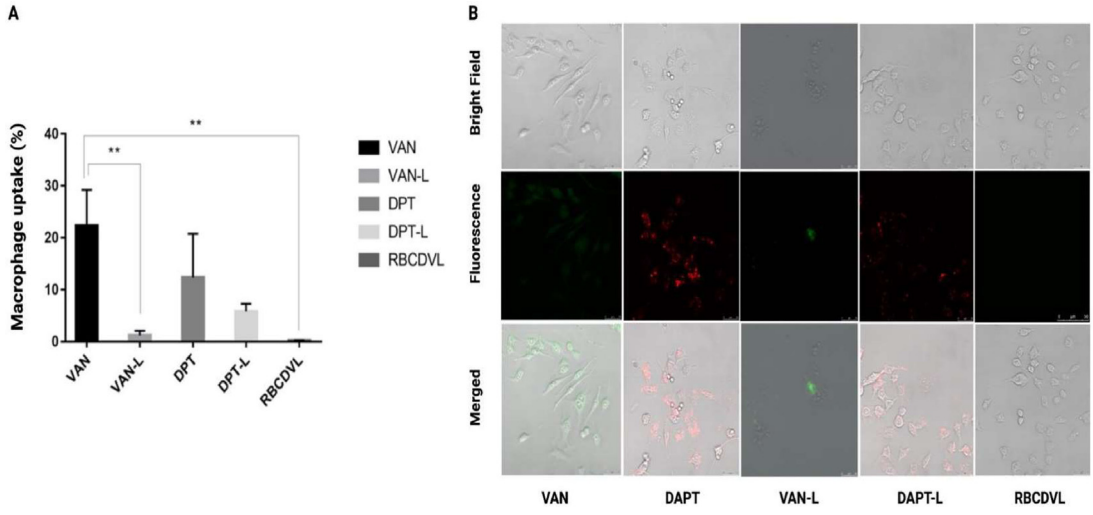

Fig. 8 – Immune-evading capabilities of VAN, DAPT, DAPT-L, VAN-L, and RBCDVL. (A) Quantification of macrophage uptake via flow cytometry and (B) CLSM images (qualitatively) showed a significant reduction in the cellular absorption of DAPT-L, VAN-L, and RBCDVL when compared to free drugs due to suppression of the scavenger receptor-mediated cellular uptake pathway. Fluorescence images of RAW264.7 were incubated with VAN stained with FAM, DAPT with DIL, and RBC conjugated with Annexin V APC for 37 °C for 2 h. The cells were washed three times with PBS prior image acquisition. Data were expressed as mean ± SD, $n = 3$.

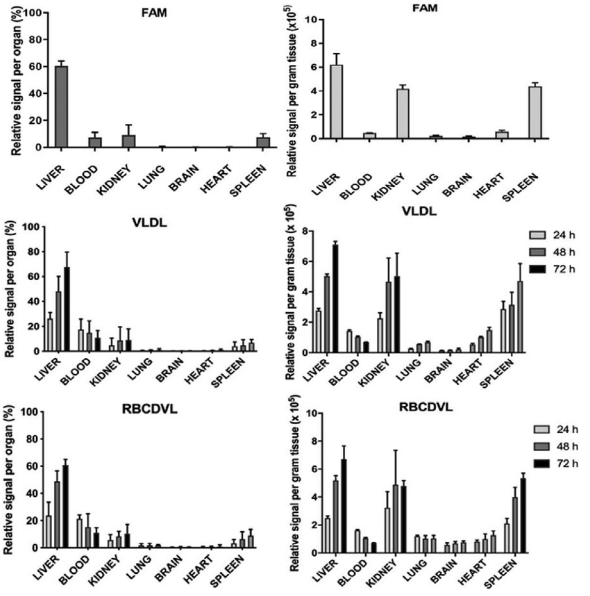

Fig. 9 – Biodistribution study of FAM and formulated DVL and RBCDVL *in vivo*. The fluorescence-labeled formulations were given to mice by intravenous injection. Organs were collected, homogenized and fluorescence counted at each time point (24, 48 and 72 h). Data were expressed as mean ± SD, $n = 4$; two-way ANOVA followed by post-hoc Tukey's multiple- comparison test.

interactions enable the recognition of opsonized formulations by phagocytes and attachment of the former to the latter. A signaling cascade is initiated, leading to actin assembly, cell surface extension formation, and particle engulfment and internalization, resulting in a "phagosome." Based on the particle surface and composition, the above events can take 30 min to several hours. As previously mentioned, complement receptors, Fc receptors, and other receptors such as scavenger receptors are involved in phagocytosis [72].

Stains of FAM and DIL were observable in the CLSM images, indicating that the VAN and DAPT free drugs and liposomal formulations may be taken up via the endolysosomal pathway. DAPT-L, VAN-L, and RBCDVL exhibited decreased cellular uptake compared to the free drugs, as observed through CLSM, and quantified using flow cytometry. As liposomes are self-assembled, the specific mechanism of the interaction pathway with the cells, either via membrane fusion or engulfment by macrophages, is not clear. In particular, enhanced drug release, hydrophobicity, cellular uptake of liposomes, and colloidal stability may result from increased rigidity [74]. High cholesterol content may have a significant impact on liposomal rigidity. A study by Wu et al. proved that cellular uptake decreased as the liposomal cholesterol content increased (40%–50%) Despite undergoing intense sonication and ultracentrifugation processes, liposomes can still be considered stable and rigid, as they can retain their morphology, which may be due to the considerable amount of cholesterol used to produce liposomes (0.306) [75]. The ability to avoid macrophages was further investigated in an *in vivo* study.

3.7. *Biodistribution*

In the biodistribution study, FAM-loaded liposomes were injected into the tail veins of the 24 rats. Eight rats were euthanized, and the kidneys, blood, liver, heart, brain, spleen and lungs were removed at designated time points of 24, 48 and 72 h after treatment. The organs were washed,

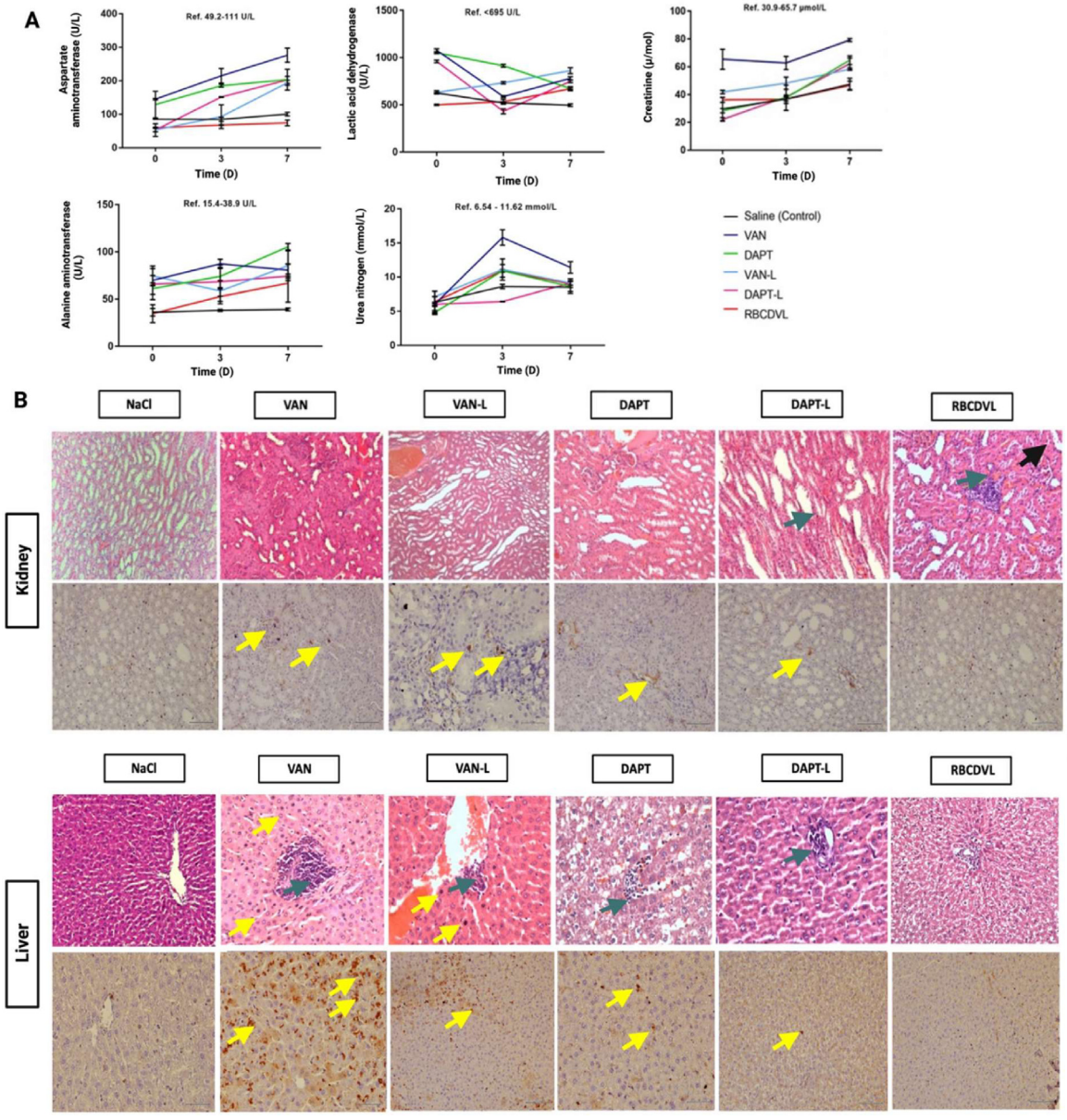

Fig. 10 – *In vivo* cytotoxicity/safety evaluation of the formulations. (A) Serum biochemical parameters of alanine aminotransferase; lactic acid dehydrogenase, aspartate aminotransferase; urea nitrogen and creatinine were observed over time in rats. Each data point represents the mean ± SD, n = 6; two-way ANOVA followed by post-hoc Tukey's multiple-comparison test. (B) The histopathological assessment of the kidney and liver on Day 3 post-treatment. Kidney & Liver (H&E and CD68, 20 x): (↗) indicates infiltration of inflammatory cells including lymphocytes; (↗) indicates granular degeneration and (↗); indicates Mesangial/Kupffer cells. Each data point represents the mean ± SD, n = 6.

weighed, and homogenized in 1 ml of PBS and then analyzed using a fluorospectrometer for fluorescence quantification. Fig. 9 depicts the liposomal content per gram of tissue and the relative signal in each organ when compared to the total liposomes. The liver and spleen, two main organs of the RES, contained the most liposomes. However, at all three time points, a significant amount of fluorescence was detected in the blood, accounting for 6% of the total body weight. Liposomes were mainly found in the blood and liver, similar to previous studies [44].

The majority of intravenously injected untargeted liposomes are eliminated from the bloodstream and are located predominantly in the spleen and liver [76–78]. As the fluorescence in the blood decreased, the signal in the liver increased, indicating that the RES acquired fluorescence from the blood. Drugs encapsulated in a double coating of liposomes with RBC membranes exhibited a significantly increased systemic circulation time compared to previous studies [43]. Greater particle stability, higher structural rigidity, and more stable cargo/dye encapsulation of the RBC-

membrane-coated liposomes resulted in a more extended circulation period than that reported in previous studies on liposome circulation in murine models [12], most of which reported attainment of insignificant blood retention within 24 h. The RBC-membrane-coated liposomes exhibited prolonged *in vivo* residence time and less toxicity, indicating that they have great potential as delivery vehicles.

3.8. *In vivo safety evaluation*

The biochemical parameters of the treatment groups were not substantially different from those of the saline control group; therefore, no apparent toxicity was observed following a single dose of the liposome formulations. In contrast to free drugs, a slight increase in the serum biochemical levels was observed in the formulation groups because the drugs were released over time. Nevertheless, the increased serum level was still lower than that of the free drugs.

On the third day after administration, histopathological evaluation was performed (Fig. 10). The dose in humans for treating susceptible pathogens was converted to the corresponding rat dose and injected accordingly. In a previous study, the human dose (mg/kg) was calculated by multiplying the animal dose (mg/kg) by the term "animal Km/human Km", while in the current study, we knew that human Km = 37 and rat Km = 6 [79,80]. Accordingly, the rat dosage (half of human dose) of DAPT was calculated as follows: 4.0 mg/kg × 37/6 = 24.67 mg/kg. Similarly, the rat dosage of VAN was calculated to be 15 mg/kg, based on the human dose being 92.5 mg/kg. Based on the optimized ratio as per an *in vitro* trial, in this study, the quantity of VAN in the liposomes for co-delivery was one-third of that in the VAN-only liposomes. When DAPT was present, the amount of VAN used could be reduced while maintaining the same clinical effect. The DAPT-L and VAN-L groups exhibited less lymphocytic infiltration and lesions than the free drug groups, as determined by hematoxylin and eosin (H&E) staining. Immunohistochemical analysis of cluster of differentiation 68 (CD68) expression was performed for validation by utilizing markers to detect abnormalities absent in normal mucosal tissue. CD68 is routinely used as a histochemical marker for macrophage/monocyte inflammatory involvement because these receptors are found in the endosomes and lysosomes of macrophages. Macrophages respond to inflammatory stimuli, leading to increased expression of CD68 because the primary function of macrophages is to eliminate pathogens and dead cells [81,82]. In the kidneys, macrophages help maintain homeostasis; however, they can also cause indirect injury to the kidneys or stimulate chronic fibrosis. Nikolic-Paterson et al. noted the presence of macrophages in individuals with renal fibrosis (CD68+), while macrophages were absent in those without renal fibrosis (CD68-) [83]. The presence of macrophages was noted in both organs (kidney and liver); nevertheless, according to the results of H&E staining, the number of macrophages present decreased in the groups treated with the NCs DAPT-L, VAN-L and RBCDVL. The presence of macrophages is intended to remodel areas of damage caused by fibrosis [84,85]. Reduced lymphocytic infiltration and tubular dilatation in the kidney and lesser lesions in the liver were more prominent in the RBCDVL group, as double coating using liposomes and RBC membranes has been reported to help protect the loaded formulation, as well as provide a more sustained release for the delivery of antibiotics [86].

4. Conclusion

The current study examined the efficacy of a DAPT-VAN combination against MRSA infections and established a novel liposomal formulation that incrated these two antibiotics in the optimal drug ratio.

A combination of egg yolk phosphatidylcholine (EPC), cholesterol, and mPEG2000 and processing factors as the as determined as the main component that will form the phospholipid bilayer of the 'stealth' liposomes. DAPT-PEG-DSPE synthesized by an amide reaction between DAPT, and NHS-PEG will be conjugated together with the other three components but excluded from the optimization step as the amount inserted will be fixed according to the previous literature. High energy ultrasonication processing method was enhanced by using I-optimal (combined) with two-factor at five levels. The effects of processing factors such as the ultrasonic intensity, sonication time, and component mixture on liposomal carrier preparation were investigated. The impact of the aforementioned factor, especially the sonication time (B), significantly influences the polydispersity index value. A favorable size of nanoliposomes can be obtained with 78.038% ultrasonic intensity and sonication time of 9.019 min. An average size of 108.13 ± 1.16 nm with a polydispersity index of 0.205 ± 0.10 was produced. The encapsulation efficiency of the coating with RBC membrane and a dual drug combination is 39.76 ± 6.17 (VAN-L) and 86.65 ± 6.13 (DAPT-L). Stability study of reconstituted RBC-coated DAPT and VAN liposomes (RBCDVL) reported some changes in physicochemical aspects such as the fading of the natural biomarker on the surface of the formulation by SDS-PAGE and agglomeration by using TEM on only when approaching 14 d above, however, showed good antibacterial activity against MRSA compared to free drugs and less toxicity in the *in vitro* and *in vivo* model. Overall, the ultrasonication process offered a helpful but straightforward method for formulating a desirable dual drug delivery liposome with reasonable encapsulation efficiency, considerable stability, and increased bactericidal effect.

Conflicts of interest

The authors declare that they have no conflicts of interest and financial competing interest.

Acknowledgements

The authors acknowledge the financial support obtained from Universiti Kebangsaan Malaysia's research university grant scheme (DCP-2017- 003/4) for experimental materials. The

funder played no part in the study's design, data collection and analysis, publication decision, or manuscript writing.

Supplementary materials

Supplementary material associated with this article can be found, in the online version, at doi:10.1016/j.ajps.2021.11.004.

REFERENCES

[1] Peters RJB, Bouwmeester H, Gottardo S, Amenta V, Arena M, Brandhoff P, et al. Nanomaterials for products and application in agriculture, feed and food. Trends Food Sci Technol 2016;54:155–64.
[2] He X, Deng H, Hwang HM. The current application of nanotechnology in food and agriculture. J Food Drug Anal 2019;27:1–21.
[3] Vimbela GV, Ngo SM, Fraze C, Yang L, Stout DA. Antibacterial properties and toxicity from metallic nanomaterials. Int J Nanomedicine 2017;12:3941–65.
[4] Hauser M, Li G, Nowack B. Environmental hazard assessment for polymeric and inorganic nanobiomaterials used in drug delivery. J Nanobiotechnology 2019;17:56.
[5] Suk JS, Xu Q, Kim N, Hanes J, Ensign LM. PEGylation as a strategy for improving nanoparticle-based drug and gene delivery. Adv Drug Deliv Rev 2016;99:28–51.
[6] Fadeel B. Hide and seek: nanomaterial interactions with the immune system. Front Immunol 2019;10:133.
[7] Sellaturay P, Nasser S, Ewan P. Polyethylene glycol-induced systemic allergic reactions (Anaphylaxis). J Allergy Clin Immunol Pract 2021;9:670–5.
[8] Bruusgaard-Mouritsen MA, Jensen BM, Poulsen LK, Duus Johansen J, Garvey LH. Optimizing investigation of suspected allergy to polyethylene glycols. J Allergy Clin Immunol 2021 S0091-6749(21)00825-3:1-21. Article in press.
[9] Kozma GT, Shimizu T, Ishida T, Szebeni J. Anti-PEG antibodies: properties, formation, testing and role in adverse immune reactions to PEGylated nano-biopharmaceuticals. Adv Drug Deliv Rev 2020;154-155:163–75.
[10] Xiong MH, Li YJ, Bao Y, Yang XZ, Hu B, Wang J. Bacteria-responsive multifunctional nanogel for targeted antibiotic delivery. Adv Mater 2012;24:6175–80.
[11] Radovic-Moreno AF, Lu TK, Puscasu VA, Yoon CJ, Langer R, Farokhzad OC. Surface charge-switching polymeric nanoparticles for bacterial cell wall-targeted delivery of antibiotics. ACS Nano 2012;6:4279–87.
[12] Jiang H, Xiong M, Bi Q, Wang Y, Li C. Self-enhanced targeted delivery of a cell wall- and membrane-active antibiotics, daptomycin, against staphylococcal pneumonia. Acta Pharm Sin B 2016;6:319–28.
[13] Mitchell MJ, Billingsley MM, Haley RM, Wechsler ME, Peppas NA, Langer R. Engineering precision nanoparticles for drug delivery. Nat Rev Drug Discov 2021;20:101–24.
[14] Algorri M, Wong-Beringer A. Antibiotics Differentially modulate lipoteichoic acid-mediated host immune response. Antibiotics (Basel) 2020;9:573.
[15] Johnston RD, Woodall BM, Harrison J, Campagna SR, Fozo EM. Removal of peptidoglycan and inhibition of active cellular processes leads to daptomycin tolerance in Enterococcus faecalis. PLoS ONE 2021;16:e0254796.
[16] Ginsburg I. Role of lipoteichoic acid in infection and inflammation. Lancet Infect Dis 2002;2:171–9.
[17] Karas JA, Carter GP, Howden BP, Turner AM, Paulin OKA, Swarbrick JD, et al. Structure-activity relationships of daptomycin lipopeptides. J Med Chem 2020;63:13266–90.
[18] Grein F, Muller A, Scherer KM, Liu X, Ludwig KC, Klockner A, et al. Ca(2+)-Daptomycin targets cell wall biosynthesis by forming a tripartite complex with undecaprenyl-coupled intermediates and membrane lipids. Nat Commun 2020;11:1455.
[19] Gray D.A., Wenzel M. More than a pore: a current perspective on the *in vivo* mode of action of the lipopeptide antibiotic daptomycin 2020;9:17.
[20] Malachowa N, DeLeo FR. Staphylococcus aureus survival in human blood. Virulence 2011;2:567–9.
[21] Malachowa N, Whitney AR, Kobayashi SD, Sturdevant DE, Kennedy AD, Braughton KR, et al. Global changes in Staphylococcus aureus gene expression in human blood. PLoS ONE 2011;6:e18617.
[22] Oliveira D, Borges A, Simoes M. Staphylococcus aureus toxins and their molecular activity in infectious diseases. Toxins (Basel) 2018;10:252.
[23] Hsieh YF, Chen TL, Wang YT, Chang JH, Chang HM. Properties of liposomes prepared with various lipids. J Food Sci 2002;67:2808–13.
[24] Kan P, Tsao CW, Wang AJ, Su WC, Liang HF. A liposomal formulation able to incorporate a high content of Paclitaxel and exert promising anticancer effect. J Drug Deliv 2011;2011:629234.
[25] Moghaddam B, Ali MH, Wilkhu J, Kirby DJ, Mohammed AR, Zheng Q, et al. The application of monolayer studies in the understanding of liposomal formulations. Int J Pharm 2011;417:235–44.
[26] Nam JH, Kim SY, Seong H. Investigation on physicochemical characteristics of a nanoliposome-based system for dual drug delivery. Nanoscale Res Lett 2018;13:101.
[27] Silva R, Ferreira H, Little C, Cavaco-Paulo A. Effect of ultrasound parameters for unilamellar liposome preparation. Ultrason Sonochem 2010;17:628–32.
[28] Li J, Wang X, Zhang T, Wang C, Huang Z, Luo X, et al. A review on phospholipids and their main applications in drug delivery systems. Asian J Pharm Sci 2015;10:81–98.
[29] Kirby C, Gregoriadis G. Dehydration-rehydration vesicles: a simple method for high yield drug entrapment in liposomes. Nat Biotechnol 1984:979–83.
[30] Sudhakar B, Krishna MC, Murthy KVR. Factorial design studies of antiretroviral drug-loaded stealth liposomal injectable: pEGylation, lyophilization and pharmacokinetic studies. Appl Nanosci 2015;6:43–60.
[31] Prabhakar K, Afzal SM, Kumar PU, Rajanna A, Kishan V. Brain delivery of transferrin coupled indinavir submicron lipid emulsions–pharmacokinetics and tissue distribution. Colloids Surf B 2011;86:305–13.
[32] Sun X, Wang C, Gao M, Hu A, Liu Z. Remotely controlled red blood cell carriers for cancer targeting and near-infrared light-triggered drug release in combined photothermal-chemotherapy. Adv Funct Mater 2015;25:2386–94.
[33] Humphries RM, Ambler J, Mitchell SL, Castanheira M, Dingle T, Hindler JA, et al. CLSI methods development and standardization working group best practices for evaluation of antimicrobial susceptibility tests. J Clin Microbiol 2018;56 e01934–17.
[34] Jones R.N., Barry A.L. Antimicrobial activity and spectrum of LY146032,a lipopeptide antibiotic, including susceptibility testing recommendations antimicrobial agents and chemotherapy 1987;31:625-9.
[35] Fuchs PC, Barry AL, Brown SD. Daptomycin susceptibility tests: interpretive criteria, quality control, and effect of calcium on *in vitro* tests. Diagn. Microbiol. Infect. Dis. 2000;38:51–8.

[36] Hajiahmadi F, Alikhani MY, Shariatifar H, Arabestani MR, Ahmadvand D. The bactericidal effect of lysostaphin coupled with liposomal vancomycin as a dual combating system applied directly on methicillin-resistant Staphylococcus aureus infected skin wounds in mice. Int J Nanomed 2019;14:5943–55.
[37] Garrod LP, Waterworth PM. Methods of testing combined antibiotic bactericidal action and the significance of the results. J Clin Pathol 1962;15:328–38.
[38] Li Y, Su T, Zhang Y, Huang X, Li J, Li C. Liposomal co-delivery of daptomycin and clarithromycin at an optimized ratio for treatment of methicillin-resistant Staphylococcus aureus infection. Drug Deliv 2015;22:627–37.
[39] Gonzalez Gomez A, Syed S, Marshall K, Hosseinidoust Z. Liposomal nanovesicles for efficient encapsulation of staphylococcal antibiotics. ACS Omega 2019;4:10866–76.
[40] Dong X, Niu Y, Ding Y, Wang Y, Zhao J, Leng W, et al. Formulation and drug loading features of nano-erythrocytes. Nanoscale Res Lett 2017;12:202.
[41] Weber C, Voigt M, Simon J, Danner AK, Frey H, Mailander V, et al. Functionalization of liposomes with hydrophilic polymers results in macrophage uptake independent of the protein corona. Biomacromolecules 2019;20:2989–99.
[42] Ahmad N, Wee CE, Wai LK, Zin NM, Azmi F. Biomimetic amphiphilic chitosan nanoparticles: synthesis, characterization and antimicrobial activity. Carbohydr Polym 2021;254:117299.
[43] Li LL, Xu JH, Qi GB, Zhao X, Yu F, Wang H. Core-shell supramolecular gelatin nanoparticles for adaptive and "on-demand" antibiotic delivery. ACS Nano 2014;8:4975–83.
[44] Hu CM, Zhang L, Aryal S, Cheung C, Fang RH, Zhang L. Erythrocyte membrane-camouflaged polymeric nanoparticles as a biomimetic delivery platform. Proc Natl Acad Sci USA 2011;108:10980–5.
[45] Zaki NM. Augmented cytotoxicity of hydroxycamptothecin-loaded nanoparticles in lung and colon cancer cells by chemosensitizing pharmaceutical excipients. Drug Deliv 2014;21:265–75.
[46] Harada Y, Yanagihara K, Yamada K, Migiyama Y, Nagaoka K, Morinaga Y, et al. *In vivo* efficacy of daptomycin against methicillin-resistant Staphylococcus aureus in a mouse model of hematogenous pulmonary infection. Antimicrob Agents Chemother 2013;57:2841–4.
[47] Dutta A, Mahapatra M, Deb M, Mitra M, Dutta S, Chattopadhyay PK, et al. Fluorescent terpolymers using two non-emissive monomers for Cr(III) sensors, removal, and bio-imaging. ACS Biomater Sci Eng 2020;6:1397–407.
[48] Ferreira Ddos S, Faria SD, Lopes SC, Teixeira CS, Malachias A, Magalhaes-Paniago R, et al. Development of a bone-targeted pH-sensitive liposomal formulation containing doxorubicin: physicochemical characterization, cytotoxicity, and biodistribution evaluation in a mouse model of bone metastasis. Int J Nanomedicine 2016;11:3737–51.
[49] Jones B, Goos P. I-optimal *versus* D-optimal split-plot response surface designs. J Qual Technol 2017;44:85–101.
[50] Lorian V, Zak O, Suter J, Bruecher C. Staphylococci, *in vitro* and *in vivo*. Diagn Microbiol Infect Dis 1985;3:433–44.
[51] Fanciullino R, Ciccolini J. Liposome-encapsulated anticancer drugs: still waiting for the magic bullet? Curr. Med. Chem. 2009;16:4361–73.
[52] Anderson MJ, Whitcomb PJ. RSM simplified: optimizing processes using response surface methods for design of experiments. 2nd ed. New York: Taylor & Francis; 2016.
[53] Richardson ES, Pitt WG, Woodbury DJ. The role of cavitation in liposome formation. Biophys J 2007;93:4100–7.
[54] Pumerantz A, Muppidi K, Agnihotri S, Guerra C, Venketaraman V, Wang J, et al. Preparation of liposomal vancomycin and intracellular killing of meticillin-resistant Staphylococcus aureus (MRSA). Int J Antimicrob Agents 2011;37:140–4.
[55] Kadry AA, Al-Suwayeh SA, Abd-Allah AR, Bayomi MA. Treatment of experimental osteomyelitis by liposomal antibiotics. J Antimicrob Chemother 2004;54:1103–8.
[56] Muppidi K, Pumerantz AS, Wang J, Betageri G. Development and stability studies of novel liposomal vancomycin formulations. ISRN Pharm 2012;2012:636743.
[57] Liu J, Wang Z, Li F, Gao J, Wang L, Huang G. Liposomes for systematic delivery of vancomycin hydrochloride to decrease nephrotoxicity: characterization and evaluation. Asian J Pharm Sci 2015;10:212–22.
[58] Francis Szoka J, Papahadjopoulos D. Procedure for preparation of liposomes with large internal aqueous space and high capture by reverse-phase evaporation. Proc Natl Acad Sci USA 1978;75:4194–8.
[59] Ghanbarzadeh S, Valizadeh H, Zakeri-Milani P. Application of response surface methodology in development of sirolimus liposomes prepared by thin film hydration technique. Bioimpacts 2013;3:75–81.
[60] Huang SM, Kuo CH, Chen CA, Liu YC, Shieh CJ. RSM and ANN modeling-based optimization approach for the development of ultrasound-assisted liposome encapsulation of piceid. Ultrason Sonochem 2017;36:112–22.
[61] Choudhury H, Gorain B, Karmakar S, Biswas E, Dey G, Barik R, et al. Improvement of cellular uptake, *in vitro* antitumor activity and sustained release profile with increased bioavailability from a nanoemulsion platform. Int J Pharm 2014;460:131–43.
[62] Calderon M, Quadir MA, Strumia M, Haag R. Functional dendritic polymer architectures as stimuli-responsive nanocarriers. Biochimie 2010;92:1242–51.
[63] Samuni AM, Lipman A, Barenholz Y. Damage to liposomal lipids: protection by antioxidants and cholesterol-mediated dehydration. Chem Phys Lipids 2000;105:121–34.
[64] Komatsu H, Saito H, Okada S, Tanaka M, Egashira M, Handa T. Effects of the acyl chain composition of phosphatidylcholines on the stability of freeze-dried small liposomes in the presence of maltose. Chem Phys Lipids 2001;113:29–39.
[65] Stark B, Pabst G, Prassl R. Long-term stability of sterically stabilized liposomes by freezing and freeze-drying: effects of cryoprotectants on structure. Eur J Pharm Sci 2010;41:546–55.
[66] Guimarães D, Noro J, Silva C, Cavaco-Paulo A, Nogueira E. Protective effect of saccharides on freeze-dried liposomes encapsulating drugs. Front Bioeng Biotechnol 2019;7:424.
[67] Hua ZZ, Li BG, Liu ZJ, Sun DW. Freeze-drying of liposomes with cryoprotectants and its effect on retention rate of encapsulated ftorafur and vitamin A. Dry Technol 2003;21:1491–505.
[68] Crowe JH, Tablin F, Wolkers WF, Gousset K, Tsvetkova NM, Ricker J. Stabilization of membranes in human platelets freeze-dried with trehalose. Chem Phys Lipids 2003;122:41–52.
[69] Franze S, Selmin F, Samaritani E, Minghetti P, Cilurzo F. Lyophilization of liposomal formulations: still necessary, still challenging. Pharmaceutics 2018;10:139.
[70] Sande L, Sanchez M, Montes J, Wolf AJ, Morgan MA, Omri A, et al. Liposomal encapsulation of vancomycin improves killing of methicillin-resistant Staphylococcus aureus in a murine infection model. J Antimicrob Chemother 2012;67:2191–4.
[71] Amin K, Dannenfelser RM. *In vitro* hemolysis: guidance for the pharmaceutical scientist. J Pharm Sci 2006;95:1173–6.
[72] Baumhover NJ, Duskey JT, Khargharia S, White CW, Crowley ST, Allen RJ, et al. Structure-activity relationship of PEGylated polylysine peptides as scavenger receptor

inhibitors for non-viral gene delivery. Mol Pharm 2015;12:4321–8.
[73] Yan X, Scherphof GL, Kamps JA. Liposome opsonization. J Liposome Res 2005;15:109–39.
[74] Wu H, Yu M, Miao Y, He S, Dai Z, Song W, et al. Cholesterol-tuned liposomal membrane rigidity directs tumor penetration and anti-tumor effect. Acta Pharm Sin B 2019;9:858–70.
[75] Briuglia ML, Rotella C, McFarlane A, Lamprou DA. Influence of cholesterol on liposome stability and on *in vitro* drug release. Drug Deliv Transl Res 2015;5:231–42.
[76] Poste G, Kirsh R. Site-specific (targeted) drug delivery in cancer therapy. Biotechnology 1983:869–78.
[77] Woodle MC, Lasic DD. Sterically stabilized liposomes. Biochim Biophys Acta 1992;1113:171–99.
[78] Senior JH. Fate and behavior of liposomes *in vivo*: a review of controlling factors. Crit Rev Ther Drug Carrier Syst 1987;3:123–93.
[79] Reagan-Shaw S, Nihal M, Ahmad N. Dose translation from animal to human studies revisited. FASEB J 2008;22:659–61.
[80] Morris TH. Antibiotic therapeutics in laboratory animals. Lab Anim 1995;29:16–36.
[81] Chistiakov DA, Killingsworth MC, Myasoedova VA, Orekhov AN, Bobryshev YV. CD68/macrosialin: not just a histochemical marker. Lab Invest 2017;97:4–13.
[82] Yu X, Guo C, Fisher PB, Subjeck JR, Wang XY. Scavenger receptors: emerging roles in cancer biology and immunology. Adv Cancer Res 2015;128:309–64.
[83] Nikolic-Paterson DJ, Wang S, Lan HY. Macrophages promote renal fibrosis through direct and indirect mechanisms. Kidney Int Suppl 2014;4:34–8.
[84] Djudjaj S, Boor P. Cellular and molecular mechanisms of kidney fibrosis. Mol Aspects Med 2019;65:16–36.
[85] Panizo S, Martinez-Arias L, Alonso-Montes C, Cannata P, Martin-Carro B, Fernandez-Martin JL, et al. Fibrosis in chronic kidney disease: pathogenesis and consequences. Int J Mol Sci 2021;22.
[86] Muzykantov VR. Drug delivery by red blood cells: vascular carriers designed by mother nature. Expert Opin Drug Deliv 2010;7:403–27.